Lack of glutathione peroxidase-1 facilitates a pro-inflammatory and activated vascular endothelium

Arpeeta Sharma[1], Derek Yuen[1], Olivier Huet[1,2], Raelene Pickering[1], Nada Stefanovic[1], Pascal Bernatchez[3] and Judy B. de Haan[1]

[1]Baker IDI Heart and Diabetes Institute, Diabetic Complications Division, Melbourne, Victoria, Australia; [2]Department of Anaesthesia and Intensive Care, CHRU La Cavale Blanche, Université de Bretagne Ouest, Brest, France; [3]Department of Anesthesiology, Pharmacology and Therapeutics, University of British Columbia.

Addresses for correspondence:

Dr. Judy de Haan
Lab Head (Oxidative Stress Laboratory)
Diabetic Complications Division
Baker IDI Heart and Diabetes Institute
75 Commercial Road
Melbourne, Victoria 3004, Australia
Phone : +61(3) 8532 1520
Fax : +61(3) 8532 1100
e-mail : judy.dehaan@bakeridi.edu.au

Abstract

A critical early event in the pathogenesis of atherosclerosis is vascular inflammation leading to endothelial dysfunction (ED). Reactive oxygen species and inflammation are inextricably linked and declining antioxidant defence is implicated in ED. We have previously shown that Glutathione peroxidase-1 (GPx1) is a crucial antioxidant enzyme in the protection against diabetes-associated atherosclerosis. In this study we aimed to investigate mechanisms by which lack of GPx1 affects pro-inflammatory mediators in primary aortic endothelial cells (PAECs) isolated from GPx1 knockout (GPx1 KO) mice. Herein, we demonstrate that lack of GPx1 prolonged TNF-α induced phosphorylation of P38, ERK and JNK, all of which was reversed upon treatment with the GPx1 mimetic, ebselen. In addition, Akt phosphorylation was reduced in GPx1 KO PAECs, which correlated with decreased nitric oxide (NO) bioavailability as compared to WT PAECs. Furthermore, IκB degradation was prolonged in GPx1 KO PAECS suggesting an augmentation of NF-κB activity. In addition, the expression of vascular cell adhesion molecule (VCAM-1) was significantly increased in GPx1 KO PAECs and aortas. Static and dynamic flow adhesion assays showed significantly increased adhesion of fluorescently labeled leukocytes to GPx1 KO PAECS and aortas respectively, which were significantly reduced by ebselen treatment. Our results suggest that GPx1 plays a critical role in regulating pro-inflammatory pathways, including MAPK and NF-κB, and down-stream mediators such as VCAM-1, in vascular endothelial cells. Lack of GPx1, via effects on p-AKT also affects signaling to eNOS-derived NO. We speculate based on these results that declining antioxidant defences as seen in cardiovascular diseases, by failing to regulate these pro-inflammatory pathways, facilitates an inflammatory and activated endothelium leading to ED and atherogenesis.

1. Introduction

A critical early event in the pathogenesis of cardiovascular diseases such as atherosclerosis is vascular inflammation. This inflammatory process drives a phenotypic change in the vascular endothelium from a protective state, where it maintains a non-adhesive and non-thrombogenic surface, to an activated state, characterized by increased adhesion of leukocytes[1]. The increase in leukocyte-endothelial interactions is driven mainly through the up-regulation of endothelial cell adhesion molecules, in particular vascular cell adhesion molecule-1 (VCAM-1)[2]. Up-regulation of this cellular adhesion molecule is induced by pro-inflammatory cytokines, such as tumor necrosis factor (TNF-α) and reactive oxygen species (ROS), both of which are prominent in the inflammatory environment. TNF-α and ROS induce adhesion molecule gene expression via the activation of several signaling pathways[3, 4]. Most importantly, TNF-α and ROS have been shown to activate the MAPK pathway, in particular extracellular signal-regulated kinase 1/2 (ERK1/2), c-Jun N-terminal kinase (JNK) and P38, as well as the redox-sensitive transcription factor, nuclear factor-κB (NF-κB)[3]. In addition, TNF-α can directly stimulate an increase in ROS production in endothelial cells[5]. Consequently, the activation of these pathways promotes vascular adhesion molecule expression and resultant vascular inflammation and dysfunction.

In addition to vascular inflammation, endothelial dysfunction is driven by compromised nitric oxide (NO) bioavailability, which is a well-recognized contributor to the initiation and progression of atherosclerosis. NO, produced in endothelial cells by constitutively expressed endothelial nitric oxide synthase (eNOS), exerts its protective vascular effects by limiting ROS and adhesion molecule expression. The activity of eNOS is greatly influenced by its phosphorylation status at a critical serine residue at position 1177 by protein kinase B (Akt), which in turn is sensitive to oxidative stress[6, 7]. During inflammation, the activation of inflammatory pathways and the increase in ROS result in scavenging of NO by superoxide, resulting in the production of another potent ROS, peroxynitrite. This results in the overall downregulation of eNOS function, thereby reducing eNOS-derived NO and its beneficial protective effects[8].

In order to maintain vascular homeostasis, the production of ROS is balanced by the activities of antioxidant enzymes, such as glutathione peroxidase (GPx),

superoxide dismutase (SOD), catalase, and peroxiredoxins. GPx1 is the most abundant isoform of the selenocysteine-containing GPx protein family, and is responsible for the detoxification of hydrogen peroxide, lipid peroxides and peroxynitrites, ROS species known to damage DNA, lipids and proteins respectively. Mounting evidence now supports an important role for GPx1 in the protection against various cardiovascular pathologies. For example, in humans, GPx1 activity was shown to be a strong and independent risk factor for cardiovascular events, both in diabetes and coronary artery disease settings[9, 10]. In experimental models, GPx1 deficiency led to endothelial dysfunction, impaired angiogenesis, and increased infarct size and vascular permeability following ischemia/reperfusion injury[11, 12]. Moreover, recent data from our laboratory[13] and others[14] have demonstrated that lack of GPx1 confers susceptibility to atherosclerosis in diabetic and hyperlipidemic settings respectively. In a recent study by Lubos et al.,[15] in human endothelial cells silenced for GPx1 expression, it was demonstrated that lowering of GPx-1 activity accelerates oxidative stress and augments NF-κB and JNK activation. Collectively, these studies strengthen the notion that GPx1 plays a major role in vascular homeostasis.

There is a strong clinical need for the development of novel antioxidants to lessen atherosclerotic burden. We have previously suggested that a targeted antioxidant strategy that augments endogenous antioxidant defences is more likely to succeed clinically in reducing atherogenic burden than vitamins such as vitamins C and E[16]. Our laboratory has focused on the cardiovascular protection afforded by a lipid-soluble low molecular weight seleno-organic GPx mimetic, ebselen (Eb). Indeed, we demonstrate a significant reduction in atherosclerosis and pro-inflammatory mediators after treatment of diabetic mice with ebselen [17, 18].

In the current study, we further investigate the role of GPx-1 in modulating inflammatory pathways that contribute to atherogenesis in primary aortic endothelial cells (PAEC) isolated from wild type (WT) and GPx-1 knockout (KO) mice. Additionally, we investigate leukocyte-endothelial cell interactions ex-vivo in aortas from GPx1 KO mice and the effect of ebselen on these pro-inflammatory pathways and interactions. We now demonstrate that lack of GPx-1 results in sustained activation of the MAPK and NF-κB pathways, and increased leukocyte adherence to the vascular endothelium, all of which

are rescued with ebselen treatment. Additionally, lack of GPx1 reduces AKT signalling and NO bioavailability. We discuss our findings in light of the impact of reduced antioxidant defense, and in particular, GPx1, on the vascular endothelium and endothelial dysfunction as well as the therapeutic benefits of augmenting GPx1-like defenses.

2. Methods

2.1. Animals

All animal experiments were approved by the Alfred Medical Research and Education Precinct (AMREP) animal ethics committee and investigations conformed to National Health and Medical Research Council (NHMRC; Australia) guidelines. GPx1 KO and WT mice were bred at the AMREP Precinct Animal Centre (PAC). GPx1 KO mice were bred onto the C57/BL6J background (10 generations). WT mice of the same background were generated via Mendelian segregation through the mating of heterozygous C57/BL6J GPx-1 and maintained as a separate line[19]. Male mice between the ages of 8-10 weeks were used for the experiments.

2.2. Isolation of primary aortic endothelial cells

PAECs were isolated from WT and GPx1 KO mice as described previously with modifications[20]. Briefly, aortas were dissected from WT and GPx1 KO mice and cleaned of peripheral fat in saline. A 22-gauge cannula was then inserted into the proximal portion and tied with a silk suture. Vessels were then perfused with Dulbecco's Modified Eagles Medium (DMEM) containing 0.2% collagenase and allowed to incubate at 37°C for 45 minutes. Next, vessels were perfused with DMEM containing 20% fetal bovine serum (FBS) and incubated at 37°C for 2 hours. Isolated cells were grown in primary endothelial cell media for 2-3 weeks until confluence. Upon confluency, WT and GPx1 KO PAECs were characterized by the gene expression of cell-specific markers, in particular endothelin A (ETA), endothelin B (ETB), smooth muscle actin (SMA), platelet endothelial cell adhesion molecule (PECAM-1) and GPx1. Additionally, the protein expression of GPx1 was confirmed by Western Blot.

2.3. Cell culture

WT and GPx1 KO PAECs were grown in EGM-2 media (Lonza) supplemented with 10% FBS at 37°C in 5% CO_2. Experiments were performed on cells from passages 3 to 8. Upon 90% confluency, cells were serum starved for 8 hrs followed by stimulation with TNF-α (20ng/ml) for 15, 30 and 60 minutes. For analysis of VCAM-1 expression, cells were not serum starved prior to exposure to 20ng/ml TNF-α which was increased to 6hr. In some experiments, cells were treated with 0.01μM ebselen for 15, 30 or 60 min which included pre-treatment for 30 min. In previously published studies in human AECs, we have established that 0.01-0.03μM ebselen was optimal for the inhibition of JNK and IKK activation, without compromising cell viability[17]. Initial experiments showed similar responses in PAEC (data not shown) and 0.01μM was chosen for all subsequent experiments.

2.4. Western Blotting

PAECs were washed twice with PBS and protein was isolated using RIPA buffer as described previously[17]. Protein concentration was determined using the BCA protein kit. Protein samples (45μg) was separated on 10% SDS-polyacrylamide gels at 150V and transferred to Nitrocellulose membranes and blocked as described previously[21]. The membranes were then incubated with either rabbit polyclonal anti-GPx1 antibody (1:100; Abcam Ltd, Cambridge, UK, ab1877), rabbit monoclonal anti-VCAM-1 (1:1000; Abcam, UK, ab29473), rabbit polyclonal anti-phospho JNK (Thr183/Tyr185) (1:1000; Cell Signaling Technology, Inc.#9251), rabbit polyclonal anti-phospho ERK (1:1000; Cell Signaling Technology, Inc.#9101), rabbit polyclonal anti-phospho P38 (1:1000; Cell Signaling Technology, Inc.#9211), rabbit polyclonal anti-phospho Akt (1:1000; Cell Signaling Technology, Inc. #9271) or rabbit monoclonal anti-phospho IKKα/β (Ser176/180) (1:1000; Cell Signaling Technology, Inc #2697) antibodies overnight at 4°C. Pierce ImmunoPure Goat anti rabbit IgG, peroxidase conjugated was used as secondary antibody for 1h. Total MAP kinase signaling was detected with appropriate antibodies (1:1000 Cell Signaling Technology, Inc. # 9252 (JNK), #9102 (ERK), #9212(p38)) and Akt (1:1000), #9272)). All membranes were hybridised with a monoclonal α-tubulin antibody (Clone B-5-1-2, Sigma, MO, USA) and visualized using

the ECL Advance Western Blotting detection kit. Signals were quantitated by densitometry using Quantity One (Bio-Rad, Hercules, CA, USA). Data are expressed relative to α-tubulin and 4 independent experiments were analysed.

2.5. Cell proliferation assays

WT and GPx1 KO PAECs were seeded in 12 well plates at a concentration of 20,000 cells/well. After overnight attachment, sub confluent monolayers were serum starved in DMEM with 0.2% FBS for 24 hours. Following which, a basal cell count was performed using the Tali image-based cytometer. Normal PAEC media was then replaced and cell counts were performed at 24 and 48 hours using the Tali image-based cytometer. In addition the 3-(4,5-dimethylthiazol-2-yl)-2,5-diphenyltetrazolium (MTT) assay (Sigma Aldrich), which detects living but not dead cells, was performed. Briefly, WT and GPx1 KO PAECs were seeded in 96 well plates at a concentration of 2,000 cells/well. After overnight attachment, sub confluent monolayers were serum starved in DMEM with 0.2% FBS for 24 hours. Following which, the media was replaced with normal PAEC media for a further 24 or 48 hours. MTT (5mg/ml) dissolved in DMEM was then added to the wells and incubated for 4 hours. The media was then aspirated from the adherent cells and 100µl DMSO/isopropanol was added to the wells to dissolve the formazen crystals. The plate was then read on the Biorad plate reader at 570nm.

2.6. In vitro and Ex vivo vessel leukocyte-adhesion assays.

Monocyte-endothelial interactions were determined by performing in vitro static cell adhesion assays as described previously by our group (ref). Briefly, WT and GPx1 KO PAECs were treated with TNF-α (1ng/ml) in the presence or absence of 0.01µM ebselen (30 minute pre-treatment). In the meantime, human monocytic THP-1 cells were labeled with the CellVue Burgundy fluorescent labeling kit (Affymetrix) as per the manufacturer's instructions and incubated with treated PAECs for 20 minutes at 37°C. Thereafter, PAECs were washed twice with phosphate-buffered saline (PBS), fixed with 10% NBF and plates were scanned using an Odyssey infra-red scanner. Fluorescence intensity (700nm) of adherent THP-1 cells was quantified.

Leukocyte-endothelial interactions were determined ex vivo by performing dynamic flow adhesion assays as described previously[22]. Briefly, aortas from WT and GPx1 KO mice were cleaned of peripheral fat in pre-warmed Krebs buffer. Aortas were then incubated with TNF-α (5ng/ml) in the presence or absence of ebselen (100µg/ml) for 4 hours. Vessels were then carefully mounted on each end of a cannula in a vessel chamber containing pre-warmed Krebs buffer. Whole human blood (5ml/vessel) was obtained from healthy volunteers and labeled with VybrantDil (1:1000) for 10 minutes at 37°C in the dark. Labeled blood was then perfused through the vessel at a rate of 100µl/min. Labeled leukocyte adhesion to the vascular wall was visualized using a fluorescent microscope coupled to a digital camera recorder. Readings were taken at two fields along the perfused vessel for 10 second durations at the 5, 10 and 15-minute time-points.

2.7. Determination of ROS

WT and GPx1 KO PAECs were incubated in phosphate buffered saline (PBS; with Ca^{2+}/Mg^{2+}) containing Dichloro-fluorescein diacetate (DCFDA; 5µM), an intracellular probe to detect ROS, for 40 minutes at 37ºC. Following which, the cells were washed with PBS and incubated with PBS alone (control) or H_2O_2 (1mM) and placed into the Omega Fluorstar reader for fluorescence detection at 485nm excitation and 530nm emission. For L-012 assays, a chemiluminescent probe to detect superoxide, WT and GPx1 KO PAECs were incubated with Krebs buffer containing L-012 (20µM) and placed in a luminometer to detect L-012 enhanced chemiluminescence for 1 hour. Background readings were subtracted and relative chemiluminescence was quantified at 30 and 60 minutes. Amplex red for the quantification of hydrogen peroxide was determined in WT and GPx1 KO homogenates using the Amplex Red Hydrogen Peroxide/Peroxidase Assay Kit (Molecular Probes) as per manufacturer's instructions.

2.8. NO analysis

Cultured media from PAECs treated with TNF-α as indicated above in section 2.3 was collected and NO measurements were performed using a using a NO-specific chemiluminescence analyzer as described previously[23]. Results are reported as pmol of nitrite per 10^6 cells.

2.9. Statistical analysis

All data are expressed as mean ± standard error of mean (SEM). Comparison between groups were analysed by performing one-way ANOVA with Newman-Keuls post hoc testing. For the dynamic flow adhesion assay, a two-way ANOVA followed by a Bonferroni post-hoc test was performed. All statistical analyses were performed using GraphPad Prism version 6.0 (GraphPad Software, La Jolla, CA, USA). A *P* value <0.05 was considered statistically significant.

3. Results

3.1. Characterization of GPx1 KO PAECs

WT PAECs exhibited protein expression of GPx1, which was completely undetected in GPx1 KO PAECs, confirming the phenotype of these cells (Fig. 1A). RT-PCR was performed for the detection of specific endothelial genes, such as ETA, ETB and PECAM-1, in GPx1 KO and WT PAECs. WT and GPx1 KO PAECs expressed high levels of ETA, ETB and PECAM-1 (data not shown). Furthermore, both WT and GPx1 KO PAECs demonstrated abundant VE-Cadherin, a vascular endothelial specific intracellular junction protein, by immunofluorescence (Supplementary figure 3A). Importantly, as compared to vascular smooth muscle cells (SMC), WT and GPx1 KO PAECs exhibited neglible smooth muscle actin gene expression (Supplementary Figure 3B), indicating minimal contamination by SMC in the endothelial cells lines. Furthermore, GPx1 KO PAECs demonstrated significantly increased levels of endogenous ROS as detected by DCF fluorescence (a probe known to detect hydrogen peroxide, lipid peroxides and peroxynitrite [24]) and L-012 (a probe known to detect superoxide[25]) chemiluminescence as compared to WT PAECS (Figure 1B and 1C). Elevations is superoxide in GPx1 KO PAECs most likely reflect upregulation of NADPH oxidases by lipid peroxides as a consequence of reduced removal of lipid peroxides in the GPx1 KO PAECs. In addition, hydrogen peroxide concentration as detected by the amplex red assay was significantly higher in GPx1 KO PAECs as compared to WT PAECs (Figure 1D). Exposure to TNF-α (2ng/ml; 30 minutes) increased hydrogen peroxide concentration in both cells types, while pre-treatment with ebselen, a known

GPx1 mimetic[26], reduced hydrogen peroxide levels in the GPx1 KO cells (Figure 1D). Collectively, these results demonstrate that GPx1 KO have a reduced capacity to remove ROS due to the lack of GPx1 as the enzyme is known to remove hydrogen peroxide, lipid peroxides and peroxynitrites.

Cell proliferation was assessed by performing cell counts and the MTT assay after a 24 hour period of serum starvation. As seen previously in cultured GPx1 KO fibroblasts[27], GPx1 PAEC KO cells exhibited significantly reduced proliferative capacity in both assays as compared to WT PAECs (Figure 1E and Figure 1F and Supplementary figure 4A). In addition, we demonstrate reduced gene expression of proliferating cell nuclear antigen (pCNA), an essential replicating factor for eukaryotic cells, in GPx1 KO PAECs compared with WT cells, as well as in human aortic endothelial cells (HAECs) silenced for GPx1 with siRNA to GPx1 (Supplementary figure 4B and 4C). Together, these data support the notion that lack of GPx1 leads to slower proliferation of cells.

3.2. Prolonged activation of inflammatory pathways in GPx1 KO endothelial cells is rescued with ebselen pre-treatment

To determine if a lack of GPx1 alters TNF-α induced MAPK signaling pathways, we stimulated WT and GPx1 KO PAECs with TNF-α (20ng/ml) in a time-dependent manner and Western Blot analysis was performed to evaluate phospho-P38 (p-P38), phospho-ERK (p-ERK) and phospho-JNK (p-JNK) expression. Following 15 minutes of TNF-α exposure, expression of p-P38, p-ERK and p-JNK was significantly increased in WT and GPx1 KO PAECs (Figure 2A and 2C, 3A and 3C, 4A and 4C), however the expression levels of these proteins were significantly higher by 1.9-, 1.5- and 1.7-fold respectively in the GPx1 KO PAECs as compared to WT controls (Figure 2A and 2C, 3A and 3C and 4A and 4C). In WT PAECs, the responses returned to baseline by the 30-minute timepoint. However, lack of GPx1 prolonged the TNF-α induced phosphorylation of JNK, p38 and ERK, resulting in significantly higher expression levels after 30 and 60 minutes of exposure to TNF-α (Figure 2A and 2C, 3A and 3C, 4A and 4C) when compared with equivalently treated WT controls. Total P38 and ERK protein expression did not change throughout the time course of TNF-α treatment for each genotype (Supplementary figure 1A and 1B). Endogenous levels of total JNK were observed to be slightly elevated

(approximately 1.5 fold) in GPx1 KO cells, however the levels of total JNK did not vary with treatment within the GPx1 KO group (Supplementary figure 1D). Higher endogenous levels of JNK in GPx1 KO cells may have arisen in response to the endogenously elevated oxidative stress that occurs in these cells as shown in Figure 1B. However, importantly, the total amount of JNK signalling (ie p-JNK) is higher in the GPx1 KO PAECs. Therefore the JNK signalling ability of the GPx1 KO cell is greater than the WT at 15 and 30 min after TNF-α stimulation. Collectively, these results clearly demonstrate that inflammatory responses to TNF-α are augmented and sustained over a longer period in endothelial cells that lack GPx1.

Treatment with Ebselen (0.01μM) significantly attenuated the extent of P38 phosphorylation after 15 minutes of TNF-α treatment in both WT and GPx1 KO PAECs (Figure 2B and 2D; Supplementary Figure 2A). Similarly, the phosphorylation of ERK was significantly attenuated by ebselen after 15 min of TNF-α stimulation in both cell types (Figure 3B and 3D; Supplementary Figure 2B). However, ebselen treatment did not have an effect on WT PAECs. In contrast, ebselen treatment significantly reduced p-JNK levels in GPx1 KO cells at the 15 min time-point (Figure 4B and 4D, Supplementary Figure 2C). In addition, ebselen was able to lessen the extended prolongation of MAPK signaling in the GPx1 KO cells. This was evident by the levels of ebselen-treated phosphorylated P38 and ERK that were significantly reduced in GPx1 KO cells compared to untreated GPx1 KO cells at the 30 min time point (P38 -Fig. 2A vs 2B and Supplementary Figure 2A); ERK - Fig. 3A vs 3B and Supplementary Figure 2B). There was also a significant reduction in pJNK by ebselen at the 30 min time point compared to untreated GPx1 KO cells (Fig.4 A vs 4B and Supplementary Figure 3C). By the 60 min time point, although significant differences were still detected, the fold decrease was significantly less between ebselen treated and non-treated GPx1 KO cells for p-38, ERK or JNK (Figs 2-4 A vs B and Supplementary Figure 2).

3.3. Akt Phosphorylation and NO release is compromised in GPx1 KO PAECs

Akt plays an important role in the phosphorylation and subsequent activation of eNOS in endothelial cells. Since eNOS-derived NO and ROS are inextricably linked in the determination of endothelial function, we examined the effect of GPx1 deficiency on Akt phosphorylation and downstream NO release in WT and GPx1 KO PAECs. After 15 minutes of exposure to TNF-α, p-Akt expression was increased 7.5 fold as compared to unstimulated WT PAECs (Figure 5A and 5B). However, p-Akt expression was not affected by TNF- α stimulation in GPx1 KO PAECS (Figure 5A and 5B). The levels of p-Akt expression in WT and GPx1 KO PAECs correlated with the quantification of NO released from the endothelial cells into the media. In WT PAECs, NO release increased in a time-dependent manner with significance reached after 15 mins following stimulation with TNF-α (20ng/ml). TNF- α had no effect on NO release from GPx1 KO cells (Figure 5C). Furthermore, we examined total and phosphorylated eNOS (at the serine 1177 site) in WT and GPx1 KO PAECs in the presence of absence of TNF- α (20 minute treatment). In supplementary figure 5, we show that GPx1 KO PAECs have a lower expression of total and phosphorylated eNOS as compared to WT PAECs, which is unaffected by TNF- α treatment.

3.4. NF-kB and VCAM-1 expression is enhanced in GPx1 KO PAECs

NF-κB is a ubiquitously expressed transcription factor that is activated by ROS and TNF-α and in turn induces the expression of cellular adhesion molecules, such as VCAM-1, and potentiates the inflammatory pathway. Under basal conditions, NF-κB is maintained in an inhibitory state through its interaction with IκB. Thus we sought to investigate if a GPx1 deficiency had an effect on NFκB activation by quantifying total IκB (T-IκB) after TNF-α stimulation. In both WT and GPx1 PAECs, T-IκB protein expression decreased after 15 and 30 minutes of TNF-α exposure, indicating a release of NF-κB from its inhibitory block (Figure 6A and 6B). After 60 minutes of TNF-α exposure, T-IκB expression returned to basal levels in WT PAECs. However, at 60 mins in GPx1 KO PAECS, T-IκB expression remained significantly reduced as compared to WT cells at 60 minutes after TNF-α treatment (Figure 6A and 6B), suggesting an elongation of the pro-

inflammatory signal in the GPx1 KO cells. Furthermore, in our study, we confirm that the lack of GPx1 results in the increased gene and protein expression of VCAM-1 following exposure to TNF-α in isolated endothelial cells (Figure 6C and Figure 6E). Treatment with ebselen resulted in a significant decrease in VCAM-1 mRNA expression in both WT and GPx1 KO PAECS (Figure 6E). Although a trend of reduction of VCAM-1 protein levels were observed in WT PAECs treated with ebselen, this did not reach significance (Figure 6D). In addition, VCAM-1 gene expression was ~1.9-fold higher in GPx1 KO aortas (Figure 6F).

3.5. *GPx1 KO mice exhibit increased leukocyte-endothelial interactions*

In order to determine if the increase in adhesion molecule expression translated to increased leukocyte-endothelial interactions, we performed a dynamic flow adhesion assay in aortas isolated from WT and GPx1 KO mice. Under basal conditions, there was a trend towards an increase in the number of adherent leukocytes between WT and GPx1 KO aortas although this did not reach significance (Figure 7A). However, upon stimulation with TNF-α (5ng/ml; 4 hours), there was a significant increase in the number of leukocytes that adhered to GPx1 KO aortas as compared to the WT aortas (Figure 7A). This difference in leukocyte adhesion was more prominent after 5 and 10 minutes of blood flow, reaching a plateau at the 15-minute time point (Figure 7A). Co-incubation of aortas with ebselen for 4 hrs prior to performing the adhesion assay resulted in a significant reduction in leukocyte adhesion to GPx1 KO aortas at all time points investigated (Figure 7B). Similarly, there was a significant increase in the adhesion of fluorescently labeled monocytes to GPx1 KO PAECs compared with WT PAECs in the absence and presence of TNF-α, which was abrogated with ebselen treatment (Figure 7C and D).

4. Discussion and Conclusion

This study shows for the first time in endothelial cells specifically isolated from the aortas of GPx1 KO mice that genetic ablation of GPx1 augments pro-inflammatory pathways that contribute significantly to endothelial dysfunction and the development of cardiovascular diseases. Our conclusions are based on the following lines of evidence: 1)

We demonstrate that a lack of GPx1 prolonged TNF-α induced phosphorylation of P38, ERK and JNK. 2) Akt phosphorylation, the protein kinase responsible for eNOS activation, was reduced in GPx1 KO PAECs which correlated with decreased NO bioavailability as compared to WT PAECs. 3) IκB degradation was prolonged in GPx1 KO PAECs suggesting an increase in NF-κB activity. 4) VCAM-1 gene and protein expression was significantly increased in GPx1 KO PAECs and GPx1 KO aortas, which correlated with augmented adhesion of inflammatory cells to the endothelium *in vitro* and *ex vivo*. Importantly, we showed that addition of ebselen, a known GPx1 mimetic was able to significantly lessen the increase in inflammatory pathways and leukocyte-endothelial interactions associated with a lack of GPx1.

Previously, our group and others have established that genetic ablation of GPx1 confers susceptibility to atherosclerosis in the presence of cardiovascular risk factors such as hyperlipidemia and diabetes[13, 14]. Particularly, we showed an increase in atherogenic cellularity, as well as proinflammatory and profibrotic markers in GPx1 KO mice[13]. However, the effect of an absence of GPx1 on endothelial dysfunction, which is a known precursor to the development of atherosclerosis, was not explored. Endothelial dysfunction, characterized by reduced NO bioavailability and increased oxidative stress as was observed in our GPx1 KO PAECs, is often implicated in endothelial activation, a phenotypic change that drives the inflammatory process mainly through the surface expression of endothelial adhesion molecules. VCAM-1 is the dominant adhesion molecule responsible for leukocyte recruitment, rolling and adhesion and its expression is significantly influenced by exogenous cardiovascular risk factors prior to physical lesion development[28]. Herein, we reveal that VCAM-1 gene and protein expression is increased in the aortas as well as in endothelial cells isolated from GPx1 KO mice in the presence of the pro-inflammatory cytokine, TNF-α. We therefore postulate that TNF-α induced activation of ROS and MAPK pathways is responsible for endothelial cell activation and VCAM-1 expression in GPx1 KO PAECs. The VCAM-1 data ties in with another major finding of our study. We demonstrate for the first time direct leukocyte adhesion to the aortic endothelium of GPx1 KO mice in **real-time** using fluorescence intravital microscopy. TNF-α treatment results in increased adhesion of fluorescently labeled leukocytes, which was further exacerbated in GPx1 KO mice over

time. Endothelial cell activation and adhesion/infiltration of leukocytes to the vascular wall occurs prior to lesion development, thus our data lends credence to studies demonstrating increased atherosclerotic lesion area in diabetic and lipogenic GPx1 knockout mice[14, 17, 18].

An interesting observation emanating from our study sheds light on basal ROS levels, VCAM-1 activation and leukocyte adhesion in GPx1 deficient PAECs. The endogenous activation of VCAM-1 in the aortas and the observed increase in adherance of leukocytes seen in GPx1-deficient endothelial cell culture might be MAPK independent since the MAPK pathways were not significantly increased under basal unstimulated conditions in our GPx1 KO PAECs, suggesting that the increase in ROS under unstimulated conditions in the GPx1 PAECs may mediate its pro-inflammatory effects via other pathways. However, in response to TNF-α, the phosphorylation of P38, ERK and JNK is significantly prolonged in endothelial cells isolated from GPx1 KO mice, indicating increased activation of the MAPK pathways and their downstream targets under pro-inflammatory and pro-oxidant conditions. This finding is highly relevant to the diabetic milieu where oxidative stress is increased and in many instances, occurs as a result of a decline in antioxidant defences such as GPx1[29, 30]. Furthermore, our study is in agreement with a recent study that exhibited increased MAPK activation upon TNF-α stimulation in human microvascular endothelial cells silenced for GPx1[15]. In addition, the present study shows that the GPx1 mimetic, ebselen, is able to inhibit TNF-α-induced P38, ERK and JNK activation in the absence and presence of Gpx1. However, a study by Yoshizumi et al, revealed that ebselen reduced TNF-α-induced JNK activation, but not P38 and ERK activation[31]. This discrepancy between the two studies could be due to differences in the cell types, particularly human umbilical vein endothelial cells vs mouse PAECs, as well as the experimental design, specifically the concentration of ebselen used.

An elegant study by Oelze et al, highlighted the important role of GPx1 in aging-associated endothelial dysfunction. In their study, GPx1 deficiency was shown to exacerbate the decrease in NO bioavailability and reduction in acetylcholine induced endothelium-dependent vasodilation as well as potentiate eNOS uncoupling associated with aging[32]. Furthermore, macrophage and leukocyte markers were significantly

elevated in aged GPx1 KO mice[32]. Our study supports these findings as we demonstrate reduced NO bioavailability and increased intracellular ROS in GPx1 KO endothelial cells. Moreover, our study lends credence to a recent study by Ahwach et al, which demonstrated that GPx1 knockdown, augmented oxidative stress but not endoplasmic reticulum stress in dextrose-induced endothelial cells, an effect that was decreased in the presence of ebselen[33]. In addition, our present study sheds light on the pathways by which GPx1 deficiency leads to endothelial cell dysfunction and activation, which promotes atherogenesis. Since GPx1 is the most abundant isoform of the glutathione peroxidases that participates in the elimination of ROS and is involved in the pathogenesis of cardiovascular diseases, it is postulated that specifically upregulating the activity of this isoform or designing functionally active mimetics could confer cardiovascular protection.

5. Acknowledgements

We wish to acknowledge The Vascular Pharmacology Laboratory of Professor Jaye Chin-Dusting for use of their equipment for the real-time flow adhesion studies. JdH acknowledges support from an Australian National Health and Medical Research Council (NH & MRC) grant #1005851. AS acknowledges support of the NHMRC Early Career Fellowship. Supported in part by the Victorian Government's OIS Program. All authors declare no conflict of interest.

6. References

1. Liao, J.K., *Linking endothelial dysfunction with endothelial cell activation.* J Clin Invest, 2013. **123**(2): p. 540-1.
2. Cybulsky, M.I., et al., *A major role for VCAM-1, but not ICAM-1, in early atherosclerosis.* J Clin Invest, 2001. **107**(10): p. 1255-62.
3. Kamata, H., et al., *Reactive oxygen species promote TNFalpha-induced death and sustained JNK activation by inhibiting MAP kinase phosphatases.* Cell, 2005. **120**(5): p. 649-61.
4. Kim, H.J., et al., *Effects of PGC-1alpha on TNF-alpha-induced MCP-1 and VCAM-1 expression and NF-kappaB activation in human aortic smooth muscle and endothelial cells.* Antioxid Redox Signal, 2007. **9**(3): p. 301-7.
5. Chen, X., et al., *Role of Reactive Oxygen Species in Tumor Necrosis Factor-alpha Induced Endothelial Dysfunction.* Curr Hypertens Rev, 2008. **4**(4): p. 245-255.
6. Zgheel, F., et al., *Redox-sensitive induction of Src/PI3-kinase/Akt and MAPKs pathways activate eNOS in response to EPA:DHA 6:1.* PLoS One, 2014. **9**(8): p. e105102.
7. Hu, Z., et al., *Bidirectional actions of hydrogen peroxide on endothelial nitric-oxide synthase phosphorylation and function: co-commitment and interplay of Akt and AMPK.* J Biol Chem, 2008. **283**(37): p. 25256-63.
8. Kawashima, S. and M. Yokoyama, *Dysfunction of endothelial nitric oxide synthase and atherosclerosis.* Arterioscler Thromb Vasc Biol, 2004. **24**(6): p. 998-1005.
9. Blankenberg, S., et al., *Glutathione peroxidase 1 activity and cardiovascular events in patients with coronary artery disease.* N Engl J Med, 2003. **349**(17): p. 1605-13.
10. Hamanishi, T., et al., *Functional variants in the glutathione peroxidase-1 (GPx-1) gene are associated with increased intima-media thickness of carotid arteries and risk of macrovascular diseases in japanese type 2 diabetic patients.* Diabetes, 2004. **53**(9): p. 2455-60.
11. Forgione, M.A., et al., *Heterozygous cellular glutathione peroxidase deficiency in the mouse: abnormalities in vascular and cardiac function and structure.* Circulation, 2002. **106**(9): p. 1154-8.
12. Forgione, M.A., et al., *Cellular glutathione peroxidase deficiency and endothelial dysfunction.* Am J Physiol Heart Circ Physiol, 2002. **282**(4): p. H1255-61.
13. Lewis, P., et al., *Lack of the antioxidant enzyme glutathione peroxidase-1 accelerates atherosclerosis in diabetic apolipoprotein E-deficient mice.* Circulation, 2007. **115**(16): p. 2178-87.
14. Torzewski, M., et al., *Deficiency of glutathione peroxidase-1 accelerates the progression of atherosclerosis in apolipoprotein E-deficient mice.* Arterioscler Thromb Vasc Biol, 2007. **27**(4): p. 850-7.
15. Lubos, E., et al., *Glutathione peroxidase-1 deficiency augments proinflammatory cytokine-induced redox signaling and human endothelial cell activation.* J Biol Chem, 2011. **286**(41): p. 35407-17.

16. Hercberg, S., P. Galan, and P. Preziosi, *Antioxidant vitamins and cardiovascular disease: Dr Jekyll or Mr Hyde?* Am J Public Health, 1999. **89**(3): p. 289-91.
17. Chew, P., et al., *Site-specific antiatherogenic effect of the antioxidant ebselen in the diabetic apolipoprotein E-deficient mouse.* Arterioscler Thromb Vasc Biol, 2009. **29**(6): p. 823-30.
18. Chew, P., et al., *Antiatherosclerotic and renoprotective effects of ebselen in the diabetic apolipoprotein E/GPx1-double knockout mouse.* Diabetes, 2010. **59**(12): p. 3198-207.
19. De Haan, J.B., et al., *An imbalance in antioxidant defense affects cellular function: the pathophysiological consequences of a reduction in antioxidant defense in the glutathione peroxidase-1 (Gpx1) knockout mouse.* Redox Rep, 2003. **8**(2): p. 69-79.
20. Kobayashi, M., et al., *A simple method of isolating mouse aortic endothelial cells.* J Atheroscler Thromb, 2005. **12**(3): p. 138-42.
21. Tan, S.M., et al., *The modified selenenyl amide, M-hydroxy ebselen, attenuates diabetic nephropathy and diabetes-associated atherosclerosis in ApoE/GPx1 double knockout mice.* PLoS One, 2013. **8**(7): p. e69193.
22. Tikellis, C., et al., *Activation of the Renin-Angiotensin system mediates the effects of dietary salt intake on atherogenesis in the apolipoprotein E knockout mouse.* Hypertension, 2012. **60**(1): p. 98-105.
23. Bernatchez, P.N., et al., *Dissecting the molecular control of endothelial NO synthase by caveolin-1 using cell-permeable peptides.* Proc Natl Acad Sci U S A, 2005. **102**(3): p. 761-6.
24. Gomes, A., E. Fernandes, and J.L. Lima, *Fluorescence probes used for detection of reactive oxygen species.* J Biochem Biophys Methods, 2005. **65**(2-3): p. 45-80.
25. Sohn, H.Y., et al., *Sensitive superoxide detection in vascular cells by the new chemiluminescence dye L-012.* J Vasc Res, 1999. **36**(6): p. 456-64.
26. Sies, H., *Ebselen, a selenoorganic compound as glutathione peroxidase mimic.* Free Radic Biol Med, 1993. **14**(3): p. 313-23.
27. de Haan, J.B., et al., *Fibroblasts derived from Gpx1 knockout mice display senescent-like features and are susceptible to H2O2-mediated cell death.* Free Radic Biol Med, 2004. **36**(1): p. 53-64.
28. Nakashima, Y., et al., *Upregulation of VCAM-1 and ICAM-1 at atherosclerosis-prone sites on the endothelium in the ApoE-deficient mouse.* Arterioscler Thromb Vasc Biol, 1998. **18**(5): p. 842-51.
29. Marra, G., et al., *Early increase of oxidative stress and reduced antioxidant defenses in patients with uncomplicated type 1 diabetes: a case for gender difference.* Diabetes Care, 2002. **25**(2): p. 370-5.
30. Szaleczky, E., et al., *Alterations in enzymatic antioxidant defence in diabetes mellitus--a rational approach.* Postgrad Med J, 1999. **75**(879): p. 13-7.
31. Yoshizumi, M., et al., *Ebselen inhibits tumor necrosis factor-alpha-induced c-Jun N-terminal kinase activation and adhesion molecule expression in endothelial cells.* Exp Cell Res, 2004. **292**(1): p. 1-10.

32. Oelze, M., et al., *Glutathione peroxidase-1 deficiency potentiates dysregulatory modifications of endothelial nitric oxide synthase and vascular dysfunction in aging.* Hypertension, 2014. **63**(2): p. 390-6.
33. Ahwach, S.M., et al., *The glutathione mimic ebselen inhibits oxidative stress but not endoplasmic reticulum stress in endothelial cells.* Life Sci, 2015.

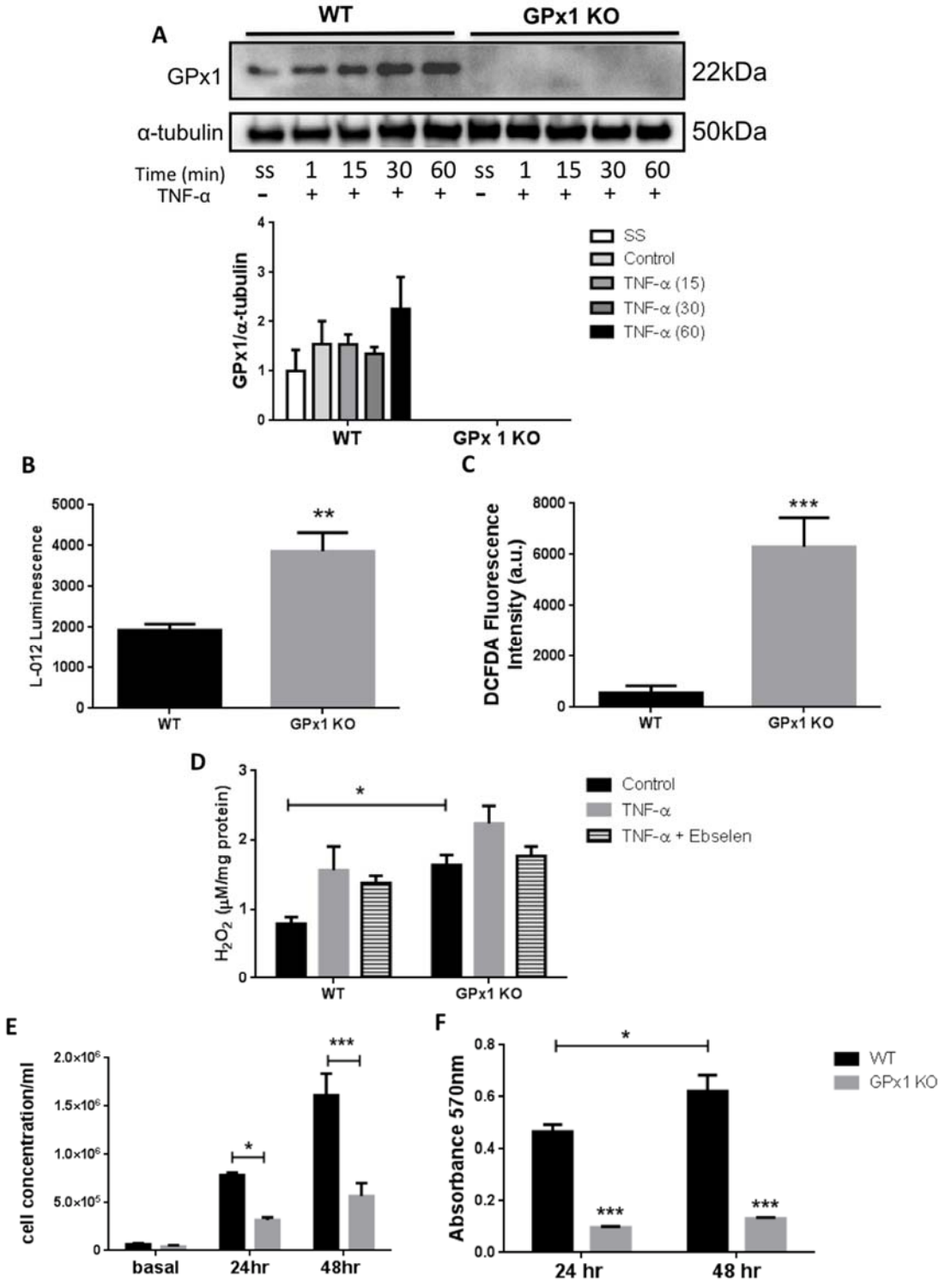

Figure 1: GPx1 KO PAECs characterization. (A) GPx1 protein expression in WT and GPx1 KO PAECs in serum starved (ss) and TNF-α treated cells after 1, 15, 30 and 60 mins of treatment. Protein was quantified relative to α-tubulin. (B) DCFDA Fluorescence intensity and (C) L-012 chemiluminescence in WT and GPx1 KO PAECs under basal conditions. (D) Hydrogen peroxide (H_2O_2) concentration in WT and GPx1 KO cells treated with TNF-α in the presence and absence of ebselen. (E) Cell proliferation and (F) MTT assay in WT and GPx1 KO PAECs after 24 and 48h of cell growth. *P<0.05, **P<0.01 and*** P<0.001 as indicated. In F, ***P<0.001 vs WT PAECs. Bars represented as mean ± SEM, n=5-8/group.

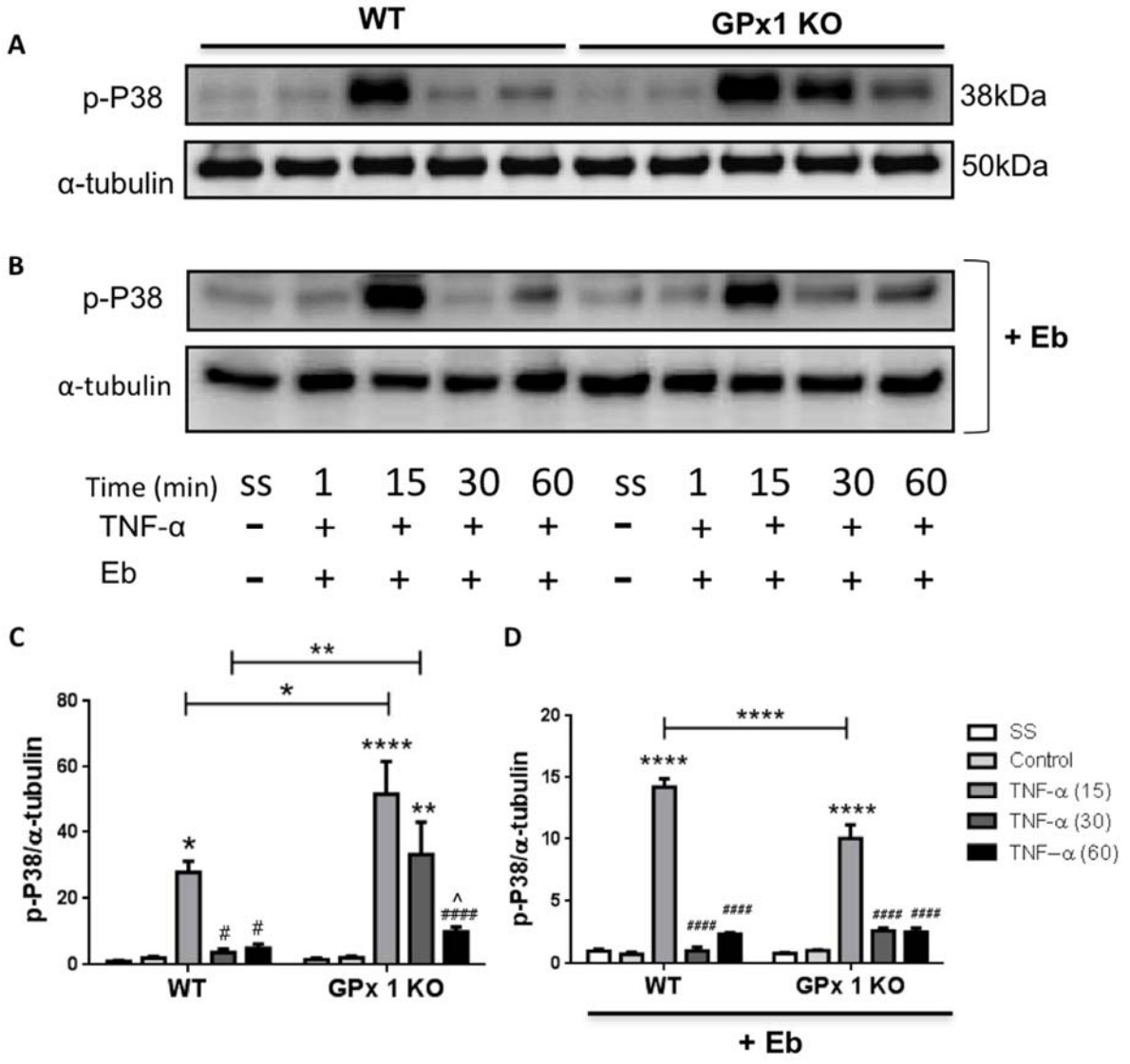

Figure 2: (A) Lack of Gpx1 potentiates TNF–α-induced increases in phosphorylation of p38. (B) In the presence of 0.01μM ebselen, phosphorylation of p38 is significantly reduced in GPx1 KO PAECs. Quantification of the Western Blots are shown in (C) and (D) respectively. *P<0.05, **P<0.01 and ****P<0.0001 as indicated. *P <0.05, **P<0.01 and ****P<0.0001 vs respective WT and GPx1 KO controls. #P<0.05 and ####P<0.0001 vs respective TNF-α (15). ^P<0.05 vs GPx1 KO TNF- α (30). Bars represented as mean ± SEM, n=4/group.

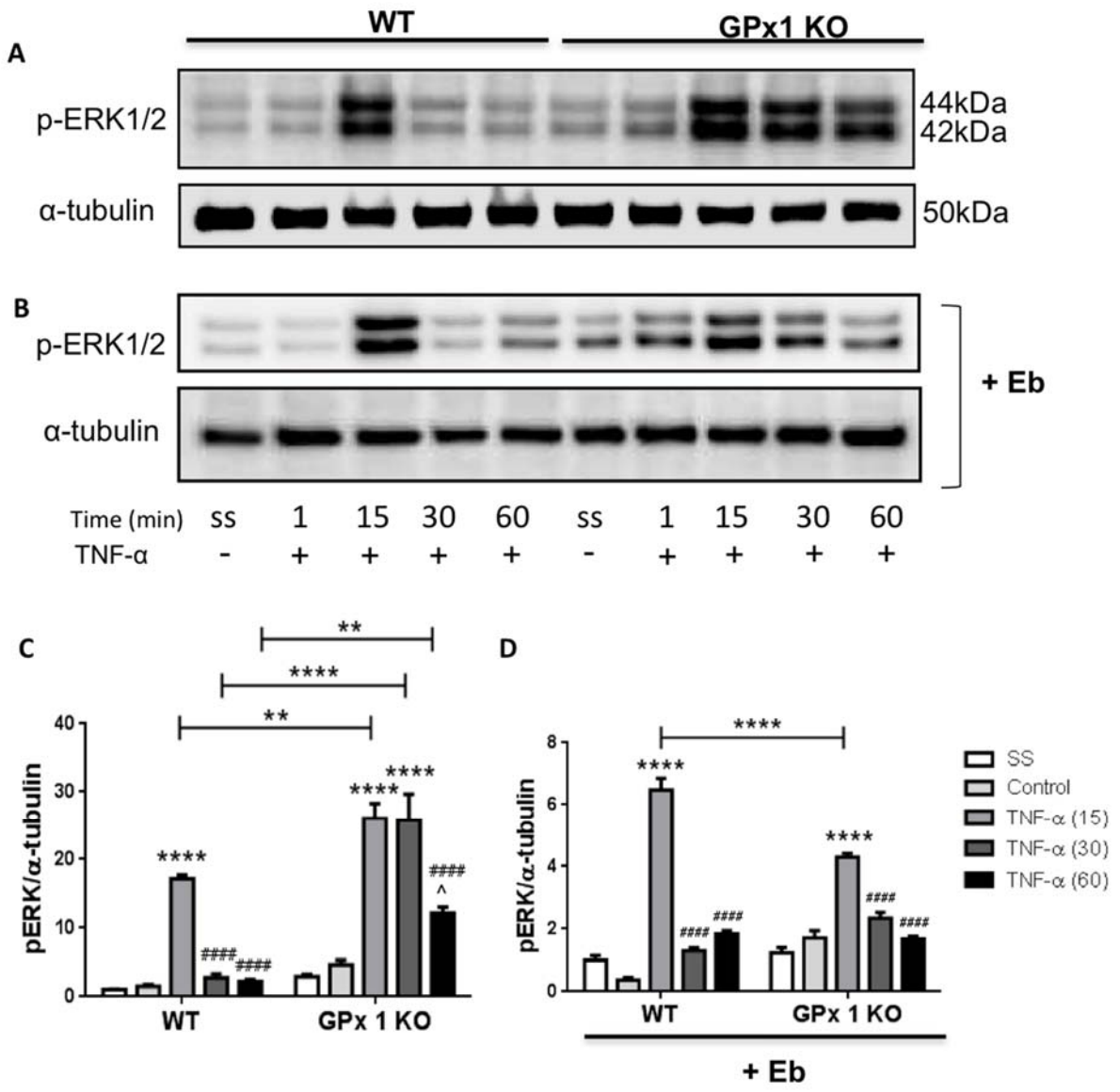

Figure 3: (A) Gpx1 deficiency augments TNF–α-induced increase in phosphorylation of pERK. (B) In the presence of ebselen (0.01μM), phosphorylation of pERK is significantly decreased in GPx1 KO PAECs. Quantification of the Western Blots are shown in (C) and (D) respectively. **P<0.01 and ****P<0.0001 as indicated. ****P<0.0001 vs respective WT and GPx1 KO controls. ####P<0.0001 vs respective TNF-α (15). ^P<0.05 vs GPx1 KO control. Bars represented as mean ± SEM, n=4/group.

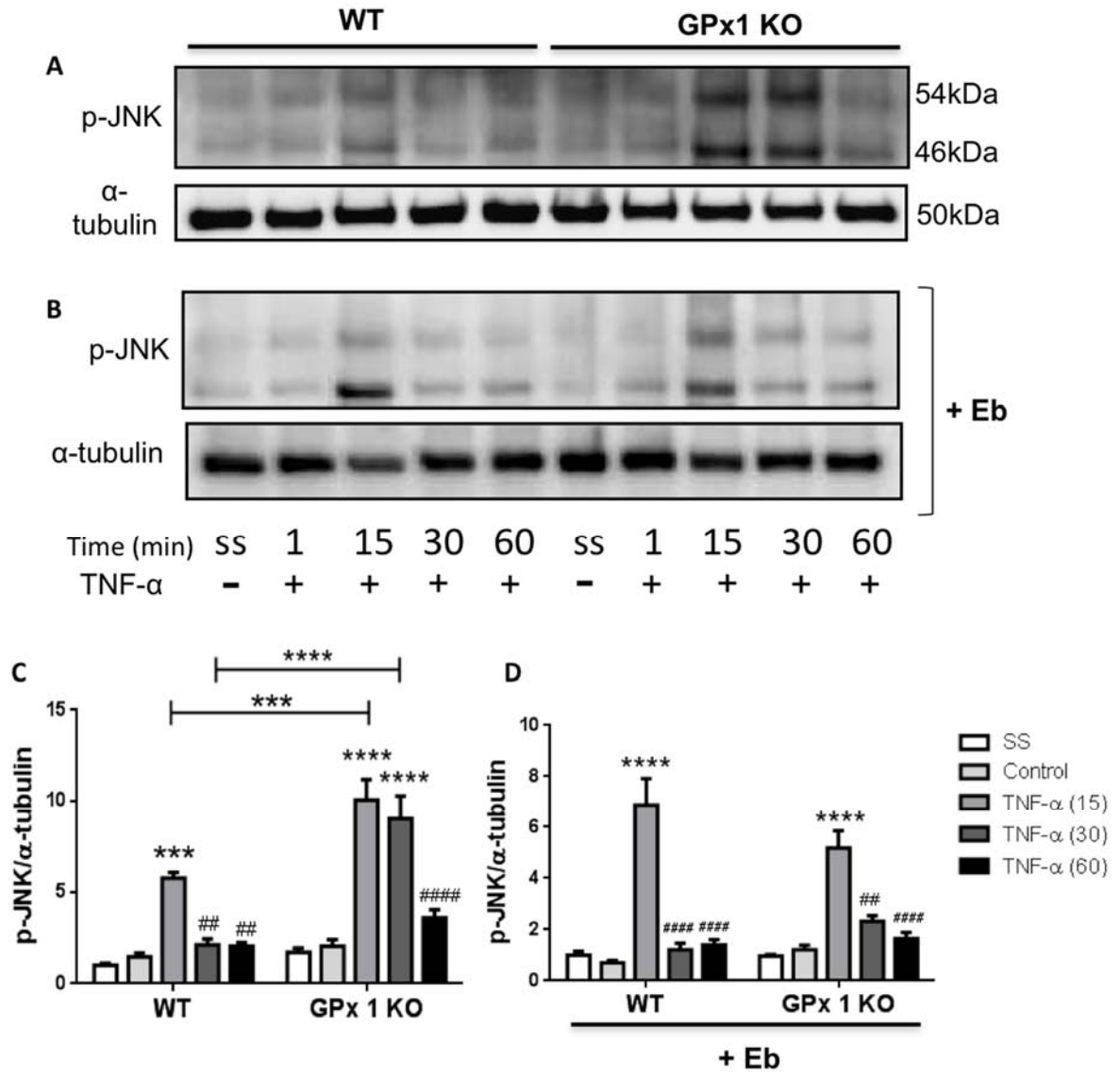

Figure 4: (A) Gpx1 KO PAECs have prolonged phosphorylation of JNK induced by TNF–α. In the presence of ebselen (0.01μM), phosphorylation of pJNK is reduced in GPx1 KO PAECs. Quantification of the Western Blots are shown in (C) and (D) respectively. ***P<0.001 and ****P<0.0001 as indicated. ***P<0.001 and ****P<0.0001 vs respective WT and GPx1 KO controls. ##P<0.01 and ####P<0.0001 vs respective TNF-α (15). Bars represented as mean ± SEM, n=4/group.

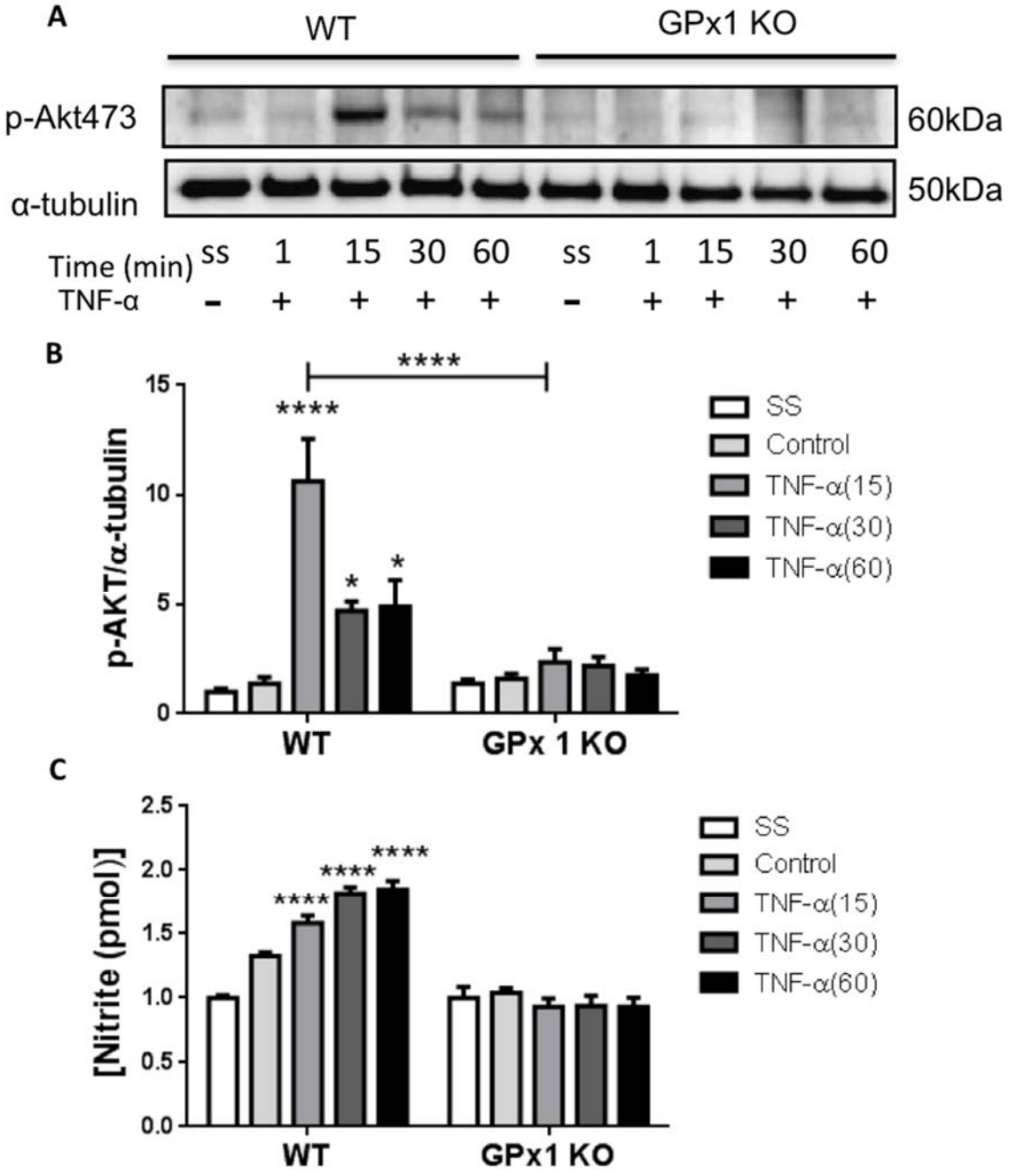

Figure 5: GPx1 KO PAECs have reduced p-Akt phosphorylation and NO levels. (A) P-Akt Western blot and (B) quantification of p-Akt in WT and GPx1 KO PAECs after TNF-α treatment is shown here. (C) Total Nitrite levels in WT and GPx1 KO PAECs stimulated with TNF- α. ****P<0.0001 as indicated. *P<0.05 and ****P<0.0001 vs WT control. Bars represented as mean ± SEM, n=4/group.

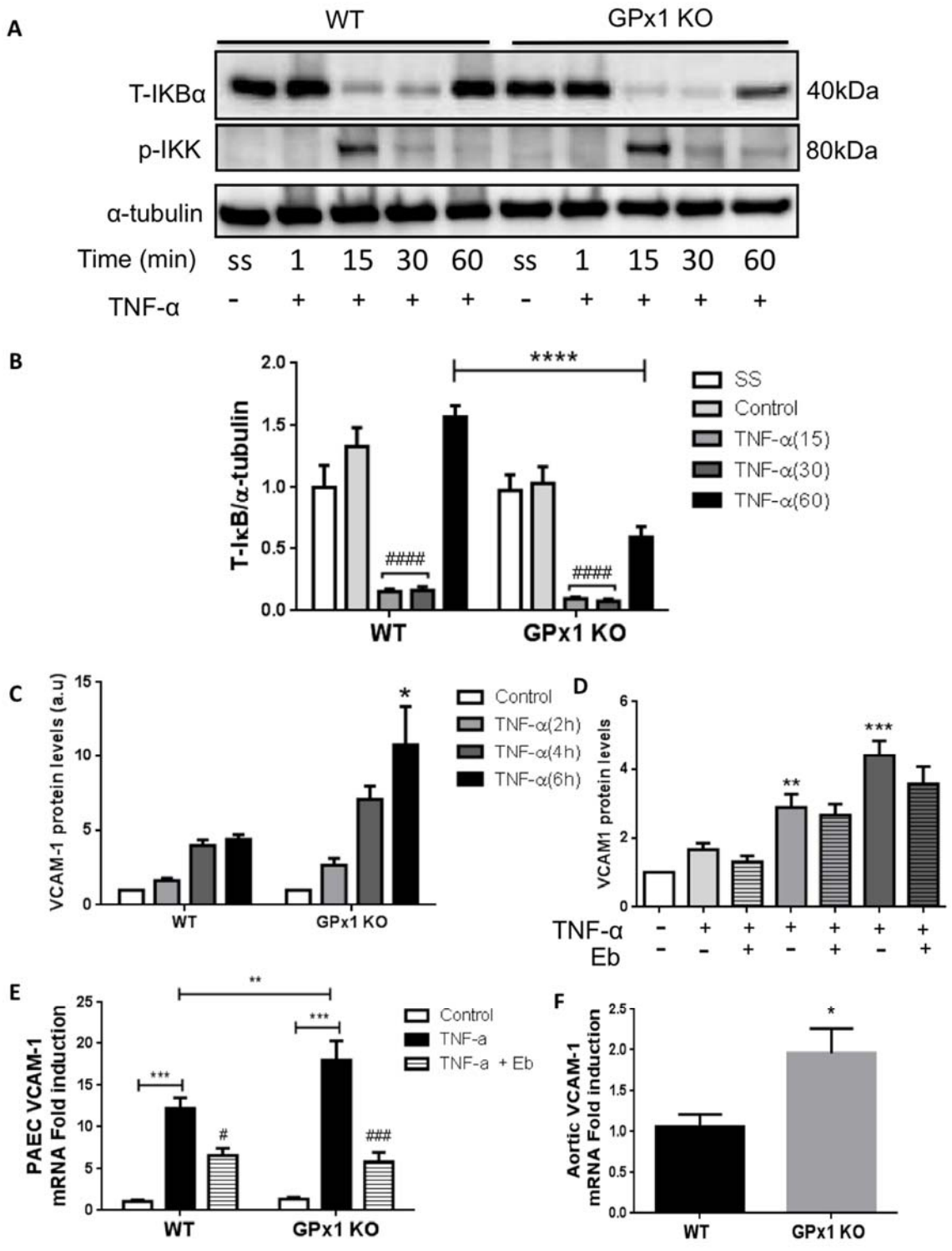

Figure 6: GPx1 KO PAECs have prolonged degradation of IκB and increased VCAM-1 expression. (A) Western blot and (B) quantification of total-IκB (T-IκB) is shown here. (C) Quantification of VCAM-1 protein levels induced by TNF-α in WT and GPx1 KO PAECs. (D) TNF-α induced VCAM-1 expression in WT PAECS in the presence of ebselen (0.01μM). (E and F) VCAM-1 gene expression in WT and GPx1 KO (E) PAECs and (F) aortas is shown here. **P<0.01, ***P<0.001 and ****P<0.0001 as indicated. *P<0.05, **P<0.01 and ***P<0.001 vs respective WT and GPx1 KO controls. #P<0.05 and ###P<0.001 vs WT and GPx1 KO in the presence of TNF-α. Bars represented as mean ± SEM, n=4/group.

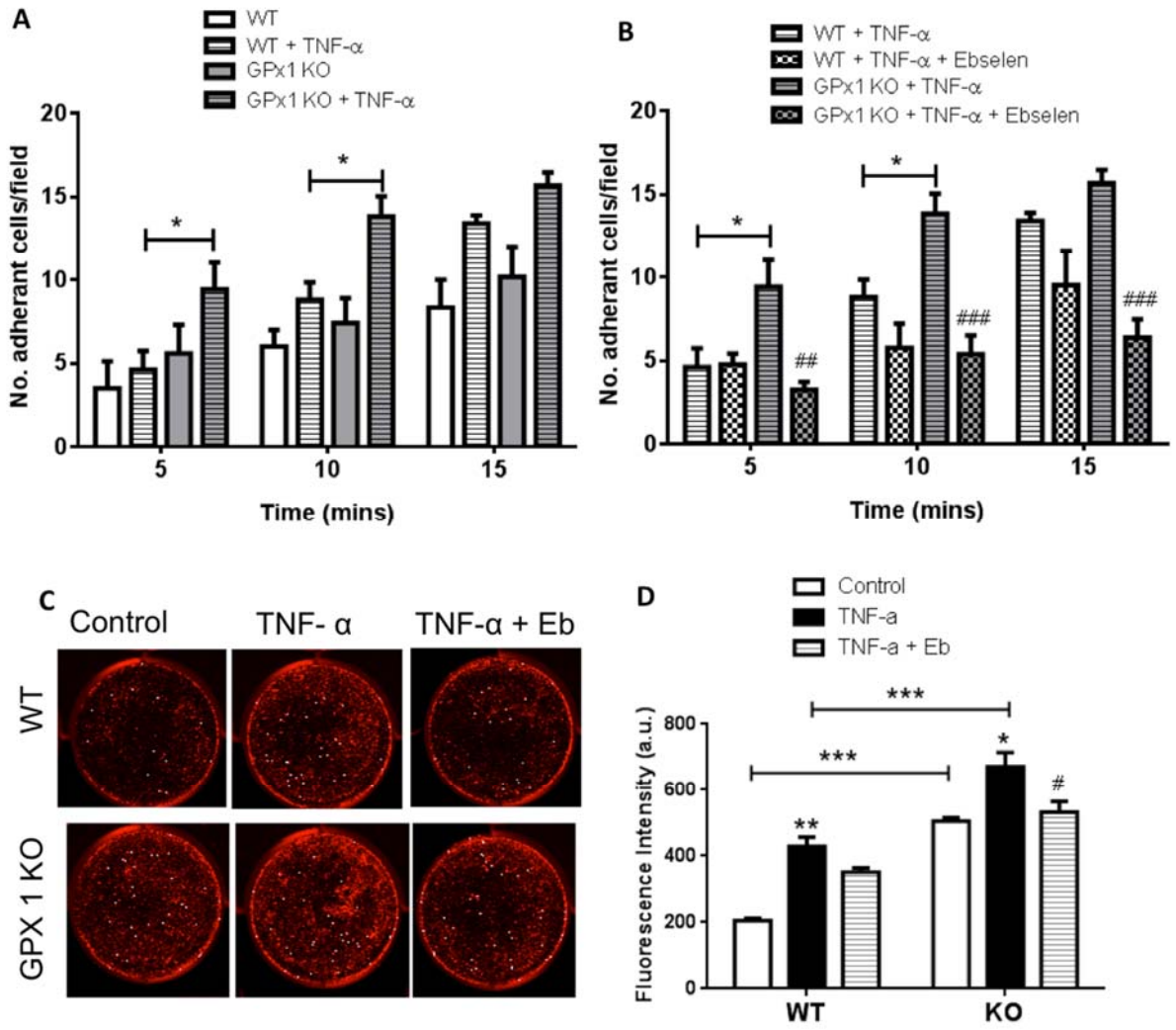

Figure 7: GPx1 KO aortas exhibit increased leukocyte-endothelial interactions. (A and B) Quantification of the number of fluorescently labeled leukocytes that adhere to the vascular endothelium in WT and GPx1 KO aortas pretreated with (A) TNF-α and (B) TNF-α + ebselen. (C) Representative images and (D) quantification of fluorescently labeled THP-1 cells to control, TNF α and TNF-α + ebselen treated WT and GPx1 PAECS. *P<0.05 and ***P<0.001 as indicated. * P<0.05 and **P<0.01 vs respective WT and GPx1 controls. #P<0.05, ##P<0.01 and ###P<0.001 vs respective GPx1 KO aortas or cells pretreated with TNF-α. Bars represented as mean ± SEM, n=5-6/group.

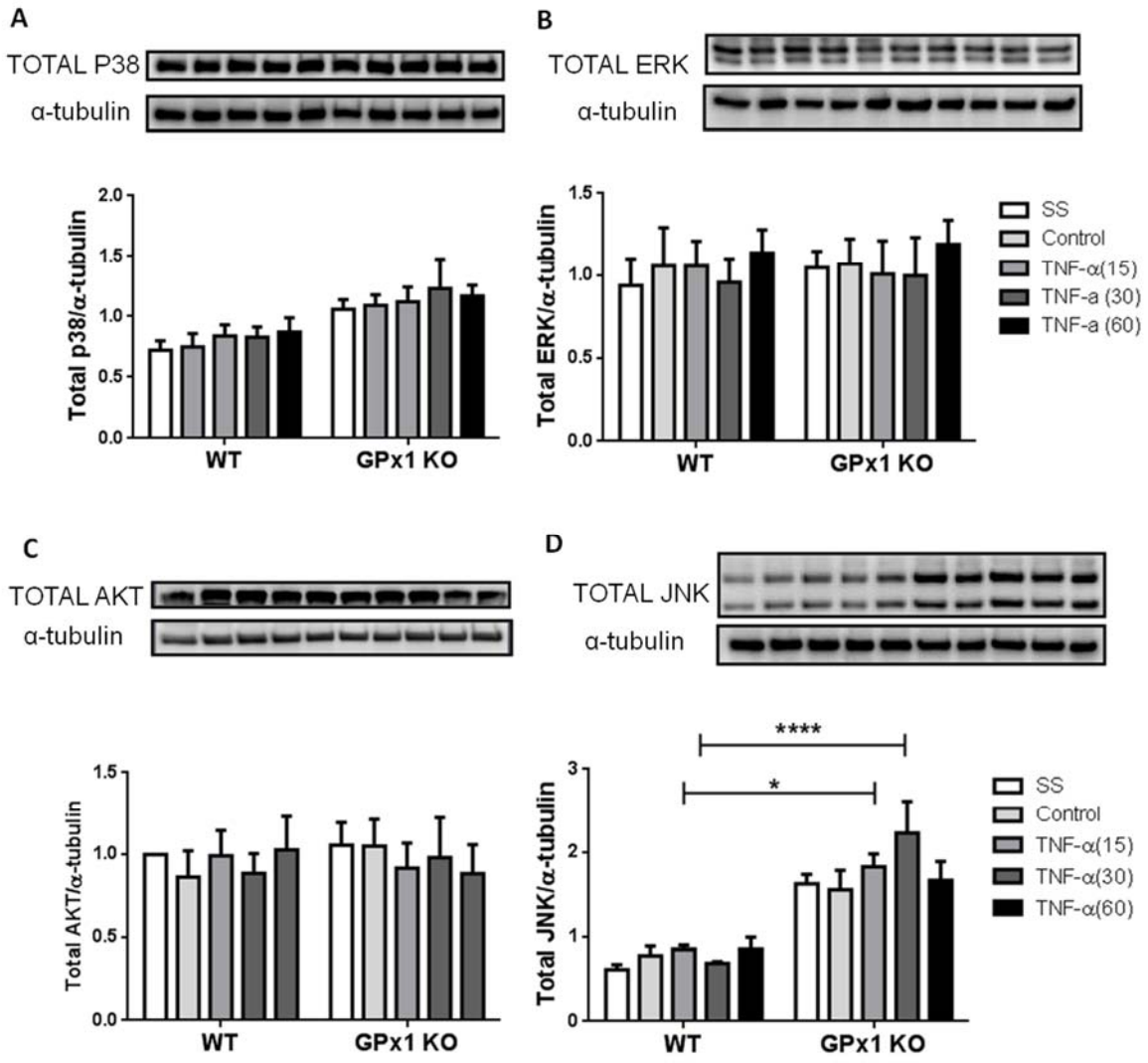

Supplementary Figure 1: Western Blot and quantification of total (A) P38, (B) ERK, (C) AKT and (D) JNK is shown here. *P<0.05 and ***P<0.001 as indicated. Bars represented as mean ± SEM, n=4/group.

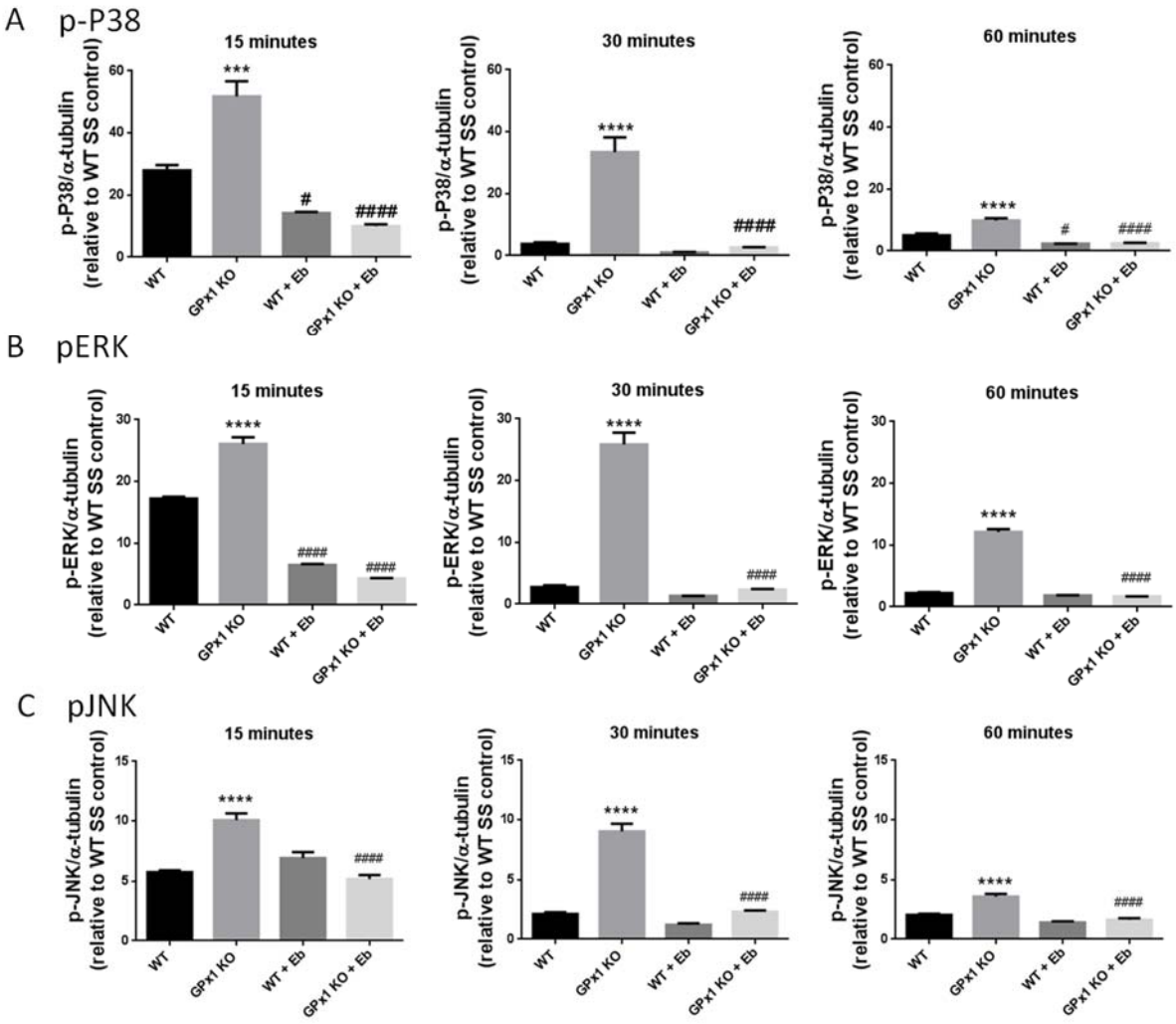

Supplementary figure 2: Fold differences in (A) p38, (B) pERK and (C) pJNK expression relative to WT serum starved (SS) controls at the 15-,30- and 60-minute time point is shown here. ***P< 0.001 and ****P<0.0001 vs WT. #P<0.05 and ####P<0.0001 vs respective controls. Bars represented as mean ± SEM, n=4/group.

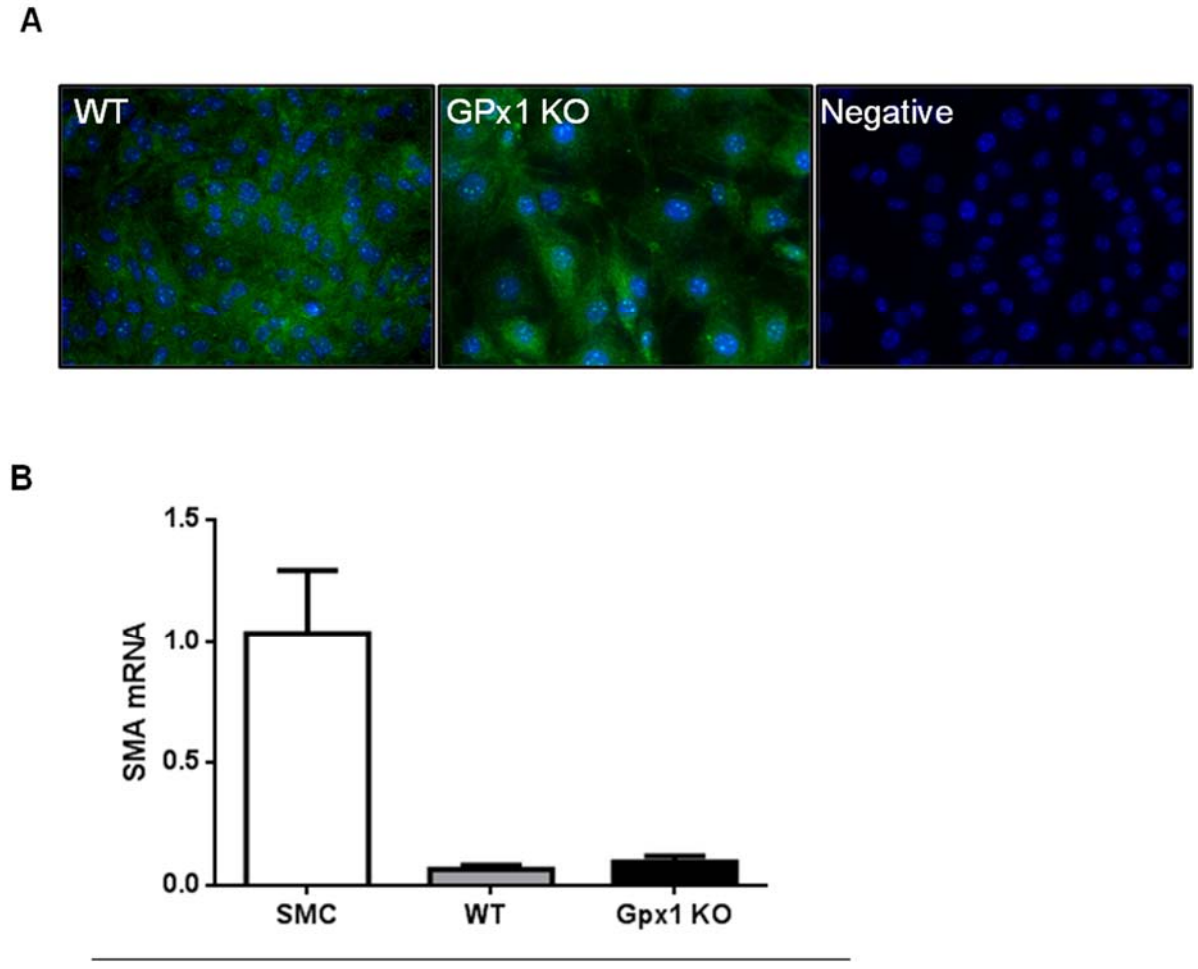

Supplementary figure 3: (A) VE-cadherin immunofluorescence in WT (panel 1) and GPx1 KO (panel 2) PAECs. No primary negative control is shown in panel 3. (B) Relative gene expression of α-smooth muscle actin (α-SMA) in WT and GPx1 KO PAECs normalized to expression levels in vascular smooth muscle cells (SMC). Bars represented as mean ± SEM, n=6-8/group.

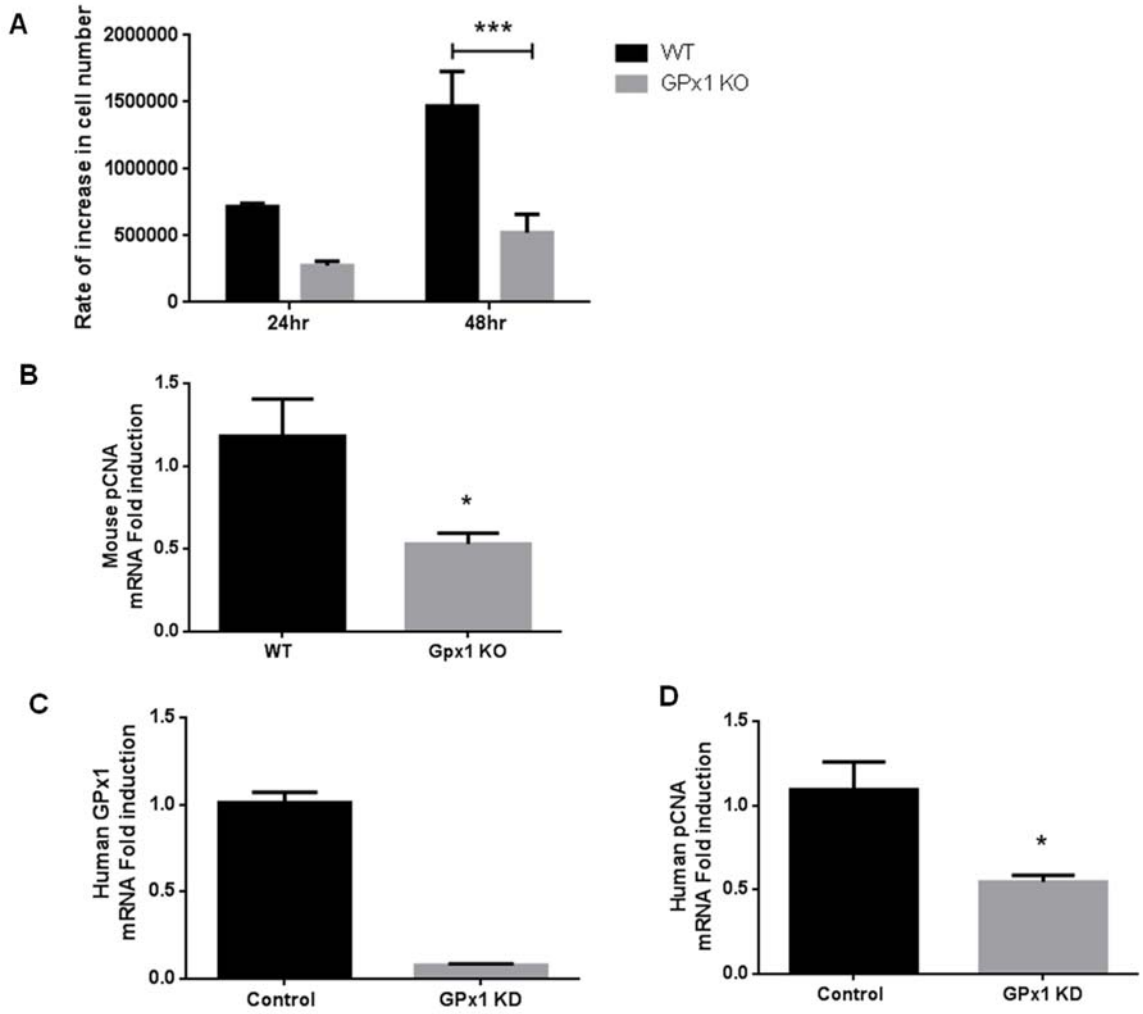

Supplementary figure 4: (A) Rate of increase in cell number after 24 and 48 hours in WT and GPx1 KO PAECs normalized to basal cell count for respective cell type. (B) Mouse pCNA gene expression in WT and GPx1 KO PAECs. (C) Human GPx1 gene expression in human aortic endothelial cells with siRNA knock down of GPx1 (GPx1 KD). (D) Human pCNA gene expression in human aortic endothelial cells with siRNA knock down of GPx1 (GPx1 KD). *P<0.05 and ***P<0.001 as indicated. Bars represented as mean ± SEM, n=6-8/group.

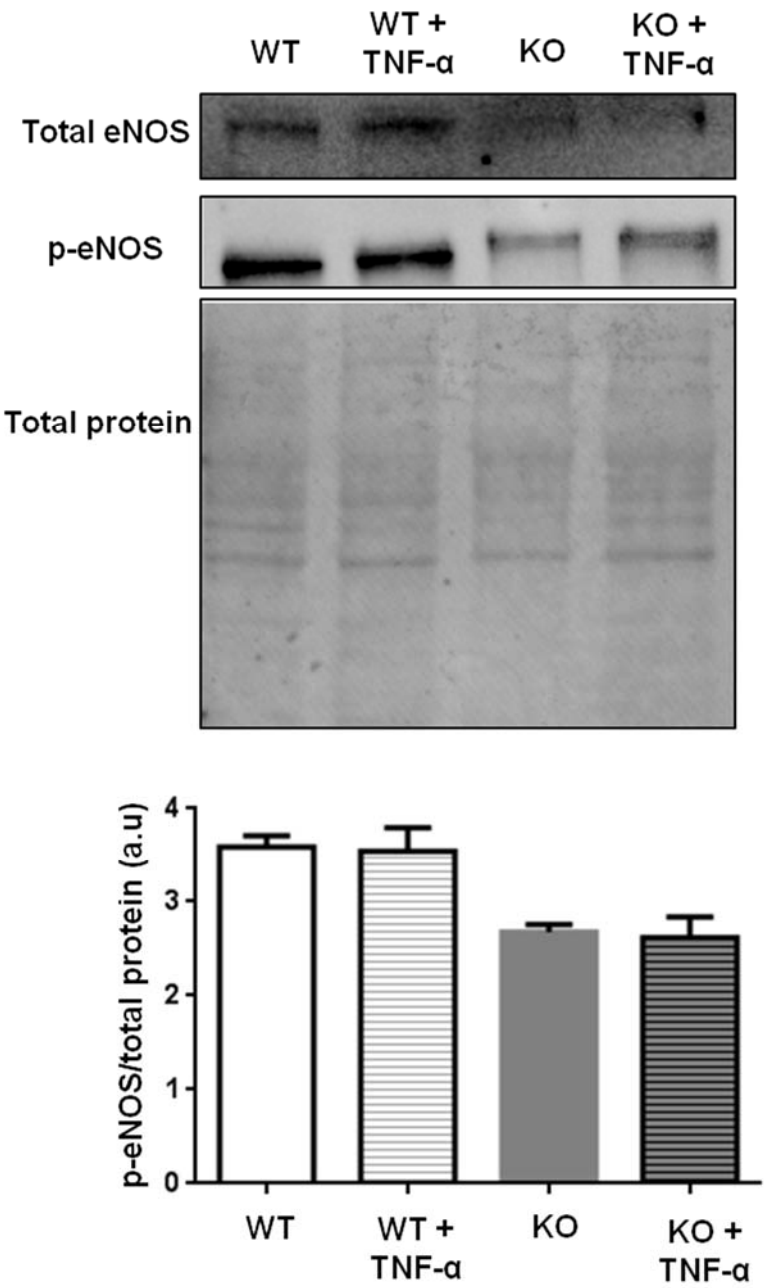

Supplementary figure 5: Western Blot demonstrating total and phosphorylated eNOS (p-eNOS) as well as total loading protein in WT and GPx1 KO PAECs in the presence and absence of TNF-α (20 minute treatment). Quantification of p-eNOS/ total protein is shown in the graph below. Bars represented as mean ± SEM, n=3/group.